

# IMPROVING IMAGING INSTRUMENT SPATIAL RESOLUTION USING SOFTWARE

(SOFTWARE SOLUTIONS FOR IMPROVING THE SPATIAL RESOLUTION OF IMAGING INSTRUMENTS FOR CUBESATS)

*Manohar Mareboyana<sup>1,2</sup>, Jacqueline Le Moigne<sup>3</sup>, Philip Dabney<sup>4</sup>*

1. Bowie State University, Bowie MD 20715
2. ASRC at NASA Goddard, Greenbelt, MD 20771
3. Software Engineering Division, NASA Goddard, Greenbelt, MD 20771
4. Biospheric Sciences Lab, NASA Goddard, Greenbelt, MD 20771

## ABSTRACT

In order to overcome spatial resolution limitations associated with physical sensor limitations when using smallsats and cubesats, we utilize an image processing technology referred to as Super-Resolution (SR). In general, software approaches are increasingly considered in connection with smaller satellites for which size, mass and power constraints limit the sensor capabilities. Being able to perform hardware vs. software trades might enable more capabilities for a lower cost. This paper describes recent experiments conducted to optimize the spatial enhancement of acquired observations using multiple sub-pixel shifted low resolution image.

**Index Terms**— super-resolution, radial basis functions

## 1. INTRODUCTION

With many future missions planning to use CubeSats and SmallSats, software approaches are increasingly considered to alleviate the size constraints of these platforms that limit the sensor capabilities.

For example, the most common CubeSat sizes are 3U and 6U, effectively limiting apertures and pupils to approximately 9 cm x 9 cm and possibly an ellipsoid of ~9cm x 18 cm. This produces a hard cutoff of spatial frequencies above 1 line/ 2.5 meters with a steep roll-off leading up to that point.

Furthermore, most low-power fine-pitch focal planes with high frame rates have low fill-factors when micro-lens arrays are eliminated to maximize the detector numerical aperture (NA) for fast optical systems and utilize the small instantaneous field of views (IFOVs) the small detector areas create. This low fill-factor produces an instantaneously under-sampled and aliased image. SR seeks to recover the higher resolution information that produces the alias and place the energy back in the appropriate location. It does this by intentionally moving the under-sampled alias image in sub-pixel pitch increments to capture all of the spatial energy delivered to the focal plane. The super resolution

(SR) techniques also accommodate non-perfect sampling pattern inputs and the inverse transform filters effectively restore the spatial power up to the spatial cutoff created by the finite active pixel IFOV/footprint.

Being able to perform hardware vs. software trades might enable more capabilities for a lower cost. In particular, a software approach is being proposed to overcome the physical sensor limitations related to spatial resolution by utilizing an image processing technology referred to as Super-Resolution (SR). SR computationally increases the spatial resolution of an image corresponding to a scene, either using a single image by retrieving information “lost” as part of the digitization and pixel integration process, or using a set of observed low resolution (LR) images of the same scene that differ by sub-pixel translations.

This paper describes the experiments that were conducted for multi-image SR and the results that were obtained using both Landsat and Worldview images demonstrating an enhancement resolution factor of 2 or 3.

## 2. VALIDATING SUPER-RESOLUTION ALGORITHMS

In the multi-image SR method, the concept is to leverage the non-redundant information contained in sub-pixel shifts low-resolution images to reconstruct the high-resolution image. As each LR image can be considered as a decimated and aliased representation of the observed scene, the non-redundant information offered by multiple LR images provides additional high frequency components compared to those that exist in a single LR image, and are used to compute the high resolution (HR) image. The multiple sub-pixel shifted images can be rapidly acquired while the observing system orbits the Earth; since the motion speed and the acquisition rate is known, the sub-pixel shifts can be easily calculated. Also, since the rate of acquisition is very high, we can reasonably assume that the calculated shift accurately represents the registration transformation between shifted low-resolution images. Figure 1 illustrates this concept.



**Figure 1** – Example of super-resolution algorithm using 9 input images, shifted from each other by a sub-pixel amount

To test this type of methods, the absolute “ground truth” validation would be to have two datasets of the same area taken at exactly the same time by two sensors having the same spectral resolution but different spatial resolution. In the absence of such ground truth datasets, we will be using the simulated framework described below and shown in Figure 2 to validate our super-resolution algorithms. Ideally test images will be created from very high-resolution (HR) images such as Worldview-1 or Worldview-2, although any image at a reasonable resolution could be used in that framework. In a first step, the original HR image is being transformed by a number of sub-pixel shifts to create the HR shifted images  $\{HR_{S1}, HR_{S2}, \dots, HR_{Sn}\}$ . Then the Point Spread Function (PSF) of the instrument being targeted is applied to each of these  $HR_{Sk}$  images. The next step is then to down-sample each of the resulting images by the amount of resolution enhancement the super-resolution algorithm is being validated for, thus creating the low-resolution (LR) images that the SR algorithm will work from or  $\{LR_{S1}, LR_{S2}, \dots, LR_{Sn}\}$ . After the Multi-Image SR algorithm has been applied, the inverse PSF is applied to the output reconstructed HR image, RHR, thus creating the final “super-resolved” image, SRI. The SRI image is compared to the original HR image using a Mean Square Error (MSE) measurement which provides an assessment of the SR algorithm that was used for the reconstruction.

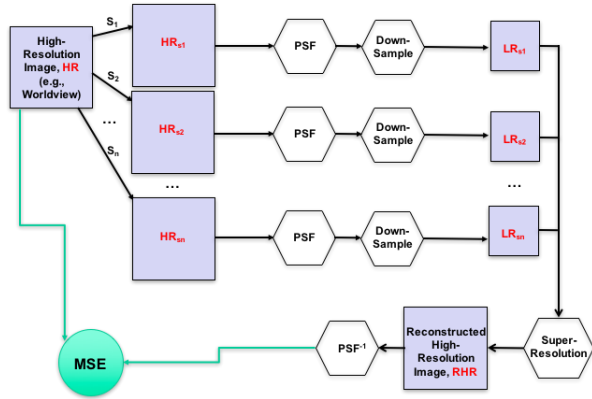


**Figure 2** – Super-Resolution Algorithms Validation Framework

### 3. SUPER-RESOLUTION FROM MULTIPLE SUB-PIXEL SHIFT IMAGES

#### 3.1 Comparison of Previously Developed Methods

Multiple approaches have been previously proposed to reconstruct the HR image based on these LR sub-pixel

images and our preliminary task has been to assess and compare these different previous approaches [1]. These are:

- Frequency Domain Approach [2] with the following characteristics:
  - Computationally efficient (using Discrete or Continuous Fourier Transform and aliasing properties to combine LR images in the SR algorithm)
  - Regularization complicated as image degradation models become complex
- Spatial Domain Approaches with the following specific methods:
  - Non-Iterative approaches including interpolation and restoration:
    - Radial Basis Function (RBF)
    - Inverse Distance Weighted (IDW)
    - Nearest Neighbor (NN)
  - Iterative Back Projection (IBP) [3]
  - Statistical Approaches such as:
    - Maximum A posteriori (MAP)
    - Maximum Likelihood (MLE)

Discrete Wavelet-Based construction (DWT) is another approach that was previously considered but because of its dyadic constraint, i.e., the resolution enhancements can only be power of 2, so it was not considered in the following experiments.

Using the testing framework described in Section 2/Figure 2, these various methods were tested using a Landsat image that was shifted (with 4 different shifts) and then down-sampled; the reconstructed HR images (by a resolution enhancement factor of 2) were then compared to the original image using the Mean Squared Error (MSE) and Peak Signal to Noise Ratio (PSNR). Table 1 shows the results of this testing for 2 sets of experiments (corresponding to 2 sets of 4 shifts).

**Table 1** – Comparative MSE Results for Various Multi-Images SR Approaches for Experiments 1 and 2

Method	Experiment 1		Experiment 2	
	MSE	PSNR dB	MSE	PSNR dB
NN (Nearest Neighbor) Interpolation	3.16	38.81	5.43	40.78
IDW (inverse Distance Weighted)	3.18	38.78	5.47	40.75
MLE (Maximum Likelihood)	3.79	38.02	4.7	41.40
IBP (Iterative Back Projection)	4.14	37.63	6.12	40.26
RBF (Radial Basis Function) Interpolation	1.28	42.73	1.53	46.28
EDRBF (Edge Directed RBF)	1.22	42.94	1.53	46.28

In these experiments, NN and RBF are the methods that consistently perform better than the other algorithms, with RBF performing best.

### 3.2 Radial Basis Functions (RBF) and Edge-Directed Radial Basis Functions (EDRBF)

Based on the previous results, our work then focused on the RBF technique and an extension of this method exploiting the directional information of edges to further improve the accuracy of RBF, the Edge-Directed Radial Basis Function (EDRBF) interpolation. The accuracy of SR depends on various factors besides the algorithm (i) number of sub-pixel shifted LR images (ii) accuracy with which the LR shifts are estimated by registration algorithms (iii) and the targeted spatial resolution of SR. In our studies, the accuracy of RBF and EDRBF will be compared with other algorithms keeping these factors constant.

Figure 3 shows the principle behind the RBF method.

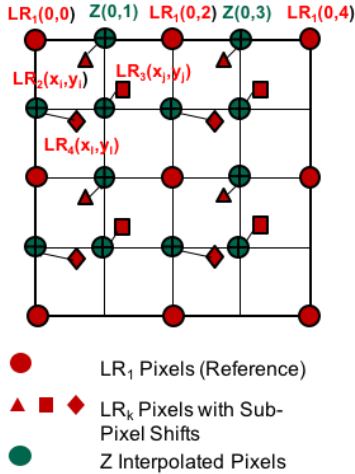


**Figure 3** – Radial Basis Functions are used to compute interpolated pixels (in green) from the sub-pixel values given by the multiple LR images (in red)

RBF are real-valued functions whose value depends on the distance from the origin, i.e.:

$$\phi(x, x_i) = \phi(\|x - x_i\|) \quad (2)$$

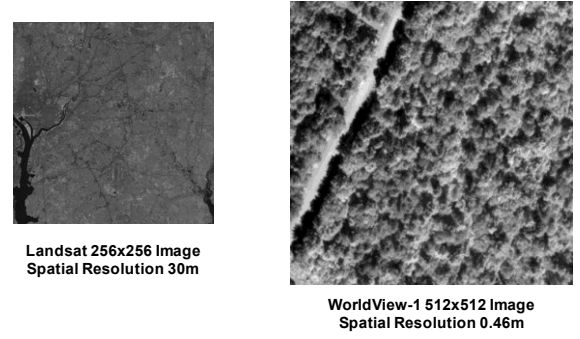
Interpolated pixels  $Z(x, y)$  values are determined from the shifted low-resolution values  $LR_k(x_i, y_i)$  as follows:

$$Z(x, y) = \sum_{(k,i)} LR_k(x_i, y_i) \phi(\|(x, y) - (x_i, y_i)\|)$$

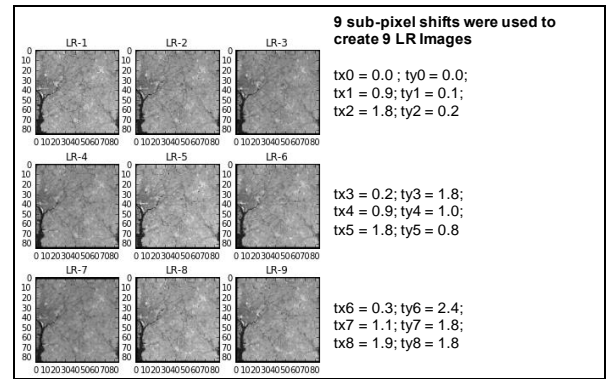
where the RBF is the Gaussian function,  $\phi(r) = e^{-\gamma r}$ . (3)

RBF and EDRBF performance was further analyzed using the 2 images shown in Figure 4 below.

Figure 5 shows the 9 shifted LR images created from the Landsat image which are used to create the super-resolution image.



**Figure 4** – Test Images Used for RBF-based SR Accuracy Assessment



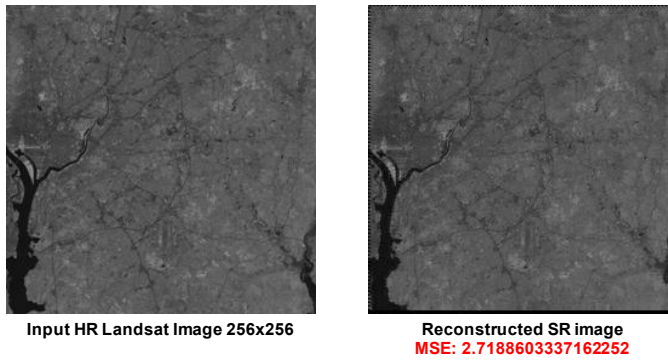
**Figure 5** – Nine 60m resolution LR sub-pixel shifted images created from the Landsat 30m image

Figure 6 shows the reconstructed SR image compared to the original Landsat image, and for this experiment, the computed Mean Square Error (MSE) is about 2.72.

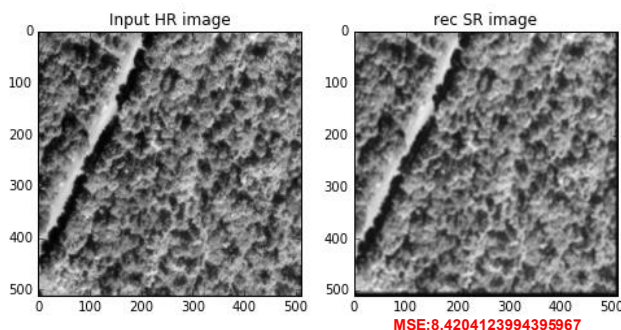
Similarly, Figure 7 shows the reconstructed HR image from a series of 9 sub-pixel shifted LR images created from the WorldView image. In this case, a Point Spread Function (PSF) based on the Wiener filter is also applied and the resulting MSE is of about 8.42.

Of course, in both cases, if the shifted LR images correspond to *whole pixel shifts* instead of sub-pixel shifts, the reconstruction is perfect with an MSE equal to 0.0.

More recent experiments using RBF, IDW, WT, and IBP have been conducted to obtain a resolution enhancement factor of 3. More results will be presented at the conference including experiments investigating the accuracy of the super-resolution as a function of the number of sub-pixel shifted images.



**Figure 6** – Comparing original and reconstructed images, for a SR resolution enhancement factor of 2, using 9 sub-pixel shifted 60 m LR images created from the Landsat image shown in Figure 4



- Using 9 Sub-Pixel Shifts:  
 $tx_1 = 0.9; ty_1 = 0.1; tx_2 = 1.8; ty_2 = 0.2;$   
 $tx_3 = 0.2; ty_3 = 1.8; tx_4 = 0.9; ty_4 = 1.0;$   
 $tx_5 = 1.8; ty_5 = 0.8; tx_6 = 0.3; ty_6 = 2.4;$   
 $tx_7 = 1.1; ty_7 = 1.8; tx_8 = 1.9; ty_8 = 1.8$
- Using PSF Wiener Filter

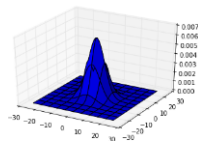


**Figure 7** – Comparing original and reconstructed images, for a SR resolution enhancement factor of 2, using 9 sub-pixel shifted 0.92 m LR images created from the WorldView 0.46m image shown in Figure 4

## 4. CONCLUSION

Experiments using various multi-image super-resolution algorithms have been conducted and RBF-based algorithms have proven to show the best results, respectively. Various assessments have been conducted for obtaining a resolution enhancement factor of 2 and have produced minimal reconstruction errors.

Additionally, recent preliminary experiments have also shown that an RBF-based algorithm could also provide that a resolution enhancement factor of 3 is feasible without introducing any significant error.

Results will be presented at the conference showing systematic assessment of both RBF and EDRBF methods with various types of test data, various numbers of sub-pixel shifted LR images, as well as various amounts of shifts. All algorithms will also be analyzed for speed and computational requirements.

## 5. ACKNOWLEDGMENTS

The authors wish to thank the Earth Science Technology Office (ESTO) Instrument Incubator Program (IIP) for funding this research.

## 6. REFERENCES

- [1] M. Mareboyana, J. Le Moigne and J.D. Bennett, “High Resolution Image Reconstruction from Projection of Low Resolution Images Differing in Subpixel Shifts,” in *Proceedings of 2016 SPIE Defense and Commercial Sensing (DCS) Conference, Computational Imaging*, edited by A. Mahalanobis et al, Baltimore, MD, April 17-21, 2016.
- [2] J. Yang and T. Huang, “Image super-resolution: Historical overview and future challenges,” Google book library 2013.
- [3] M. Irani and S. Peleg, “Improving resolution by Image Registration,” *Computer Vision Graphics and Image Processing*, Graphical Models and Image Processing, Vol. 53, No.3, May 1991.